intermediate rainfall (fig. S2), although it was weakly predictive of tree cover (table S1). It is possible that global soils data sets are insufficiently accurate or fine-scaled, but this analysis suggests that soils do not provide an alternative mechanism for explaining global bimodalities in tree cover.

Patterns of fire, tree cover, and climate are consistent with the idea that fire can function in savanna systems as a positive feedback, wherein fire suppresses tree cover (*6*–*8*) and low tree cover promotes fire spread (*1*, *9*, *10*). This feedback affects observed tree cover patterns by expanding the range of savanna beyond areas with climates that directly limit tree cover and by maintaining the bimodalities that define savanna and forest as distinct states. However, the not-infrequent incidence of fires in high–tree-cover areas of South America suggests that some dynamic change between states may be possible. Under hot, dry conditions, forest litter can carry fires; forests have only a limited capacity to recuperate from such events (*20*, *21*). These South American forests may be more subject to an ongoing process of encroachment of fire and savanna than are African forests.

The global impacts of these fire feedbacks on savanna and forest distributions are extensive (Fig. 4). If savanna and forest are alternative stable states over large parts of their range, as we argue, explicit considerations of transitions between the two are fundamental to understanding historical and future changes in biome distributions globally. C_4 grass evolution and the global expansion of savanna occurred during the Miocene, a period marked not only by aridity but also by increased rainfall seasonality (*22*). Paleoecological work suggests that contemporary savannas occurring in areas now wet enough to support forest were probably established during drier periods in Earth's history (*23*), in line with the idea that fire feedbacks promote the persistence of historical biome distributions.

Ongoing human-driven global change is likely to have major impacts on those distributions for a variety of reasons. Historical biome distributions were certainly affected by humans in some areas (*24*, *25*), but modern human activities are much more extensive and intensive. Fire exclusion experiments (*6*–*8*) and documentation of forest encroachment from around the world (*26*, *27*) provide evidence that changing burning practices and patterns through landscape fragmentation and management policy have resulted in widespread encroachment of forest into savanna. The weakening of the monsoon could compound these effects (*28*). Meanwhile, recent work has suggested that global climate change could put Amazonia at risk of severe drying (*29*) and that increased fire risk could compound these effects (*30*, *31*), potentially resulting in widespread transitions from forest to savanna. Depending on climatic context, massive areas of South America and possibly of Africa that are currently characterized by savanna and forest are potentially at risk for changes in biome state (Fig. 4). Those changes, whether at the cost of savanna or forest, are unlikely to be smooth or easily reversible.

References and Notes

1. A. C. Staver, S. Archibald, S. Levin, *Ecology* **92**, 1063 (2011).
2. C. E. Lehmann, S. A. Archibald, W. A. Hoffmann, W. J. Bond, *New Phytol.* **191**, 197 (2011).
3. M. Sankaran *et al.*, *Nature* **438**, 846 (2005).
4. G. Bucini, N. Hanan, *Glob. Ecol. Biogeogr.* **16**, 593 (2007).
5. M. Sankaran, J. Ratnam, N. Hanan, *Global Ecol. Biogeogr.* **17**, 236 (2008).
6. M. Swaine, W. Hawthorne, T. Orgle, *Biotropica* **24**, 166 (1992).
7. A. Moreira, *J. Biogeogr.* **27**, 1021 (2000).
8. W. Bond, *Annu. Rev. Ecol. Syst.* **39**, 641 (2008).
9. S. Archibald, D. Roy, B. van Wilgen, R. Scholes, *Glob. Change Biol.* **15**, 613 (2009).
10. S. Pueyo *et al.*, *Ecol. Lett.* **13**, 793 (2010).
11. R. Williams, G. Duff, D. Bowman, G. Cook, *J. Biogeogr.* **23**, 747 (1996).
12. P. G. Cruz Ruggiero, M. A. Batalha, V. R. Pivello, S. T. Meirelles, *Plant Ecol.* **160**, 1 (2002).
13. S. P. Good, K. K. Caylor, *Proc. Natl. Acad. Sci. U.S.A.* **108**, 4902 (2011).
14. E. Veenendaal, O. Kolle, J. Lloyd, *Glob. Change Biol.* **10**, 318 (2004).
15. D. Cahoon Jr., B. Stocks, J. Levine, W. Cofer III, K. O'Neill, *Nature* **359**, 812 (1992).
16. Materials and methods, as well as other supporting material, is available on *Science* Online.
17. H. Prins, H. van der Jeugd, *J. Ecol.* **81**, 305 (1993).
18. A. C. Staver, W. J. Bond, W. D. Stock, S. J. Van Rensburg, M. S. Waldram, *Ecol. Appl.* **19**, 1909 (2009).
19. S. Archibald, W. Bond, W. Stock, D. Fairbanks, *Ecol. Appl.* **15**, 96 (2005).
20. M. A. Cochrane *et al.*, *Science* **284**, 1832 (1999).
21. J. Balch *et al.*, *Glob. Change Biol.* **14**, 2276 (2008).
22. J. Keeley, P. Rundel, *Ecol. Lett.* **8**, 683 (2005).
23. T. Desjardins, A. C. Filho, A. Mariotti, C. Girardin, A. Chauvel, *Oecologia* **108**, 749 (1996).
24. K. J. Willis, L. Gillson, T. M. Brncic, *Science* **304**, 402 (2004).
25. F. E. Mayle, R. P. Langstroth, R. A. Fisher, P. Meir, *Philos. Trans. R. Soc. London Ser. B* **362**, 291 (2007).
26. D. Goetze, B. Horsch, S. Porembski, *J. Biogeogr.* **33**, 653 (2006).
27. E. Mitchard, S. Saatchi, F. Gerard, S. Lewis, P. Meir, *Earth Interact.* **13**, 1 (2009).
28. K. K. Kumar, B. Rajagopalan, M. A. Cane, *Science* **284**, 2156 (1999).
29. O. L. Phillips *et al.*, *Science* **323**, 1344 (2009).
30. Y. Malhi *et al.*, *Proc. Natl. Acad. Sci. U.S.A.* **106**, 20610 (2009).
31. G. P. Asner, A. Alencar, *New Phytol.* **187**, 569 (2010).

Acknowledgments: We thank A. Wolf, S. Batterman, and S. Rabin for manuscript feedback. Funding was provided by the Andrew W. Mellon Foundation. All data are freely available at http://modis.gsfc.nasa.gov/, http://trmm.gsfc.nasa.gov/, and www.fao.org/nr/land/soils/harmonized-world-soil-database/en/.

Supporting Online Material

www.sciencemag.org/cgi/content/full/334/6053/230/DC1
Materials and Methods
Figs. S1 and S2
Table S1
References (*32*–*37*)

28 June 2011; accepted 6 September 2011
10.1126/science.1210465

Global Resilience of Tropical Forest and Savanna to Critical Transitions

Marina Hirota,[1] Milena Holmgren,[2]* Egbert H. Van Nes,[1] Marten Scheffer[1]

It has been suggested that tropical forest and savanna could represent alternative stable states, implying critical transitions at tipping points in response to altered climate or other drivers. So far, evidence for this idea has remained elusive, and integrated climate models assume smooth vegetation responses. We analyzed data on the distribution of tree cover in Africa, Australia, and South America to reveal strong evidence for the existence of three distinct attractors: forest, savanna, and a treeless state. Empirical reconstruction of the basins of attraction indicates that the resilience of the states varies in a universal way with precipitation. These results allow the identification of regions where forest or savanna may most easily tip into an alternative state, and they pave the way to a new generation of coupled climate models.

Tree cover is one of the defining variables of landscapes, their ecological functioning, and their impact on climate. Despite insights into the effects of resource availability and disturbances on tree growth and survival (*1*–*4*), our understanding of the mechanisms determining global patterns of tree cover remains fragmented. A major question is whether tree cover will respond smoothly to climatic change and other stressors (*5*) or exhibit sharp transitions between contrasting stable states at tipping points (*6*). In some regions, forest, savanna, and treeless (barren or grassy) states have been suggested to represent alternative attractors (*7*–*9*). However, the case for multiple stable states of tree cover is largely based on models and on local observations of sharp transitions (*6*–*9*). Systematic studies of tree-cover distributions could help distinguish between hypotheses (*1*) but have been largely restricted to particular continents or biome types (*4*–*6*, *10*, *11*). To explore whether global patterns of tree abundance suggest gradual responses or, rather, alternative stable states, we

[1]Department of Aquatic Ecology and Water Quality Management, Wageningen University, Post Office Box 47, NL-6700 AA, Wageningen, Netherlands. [2]Resource Ecology Group, Wageningen University, Post Office Box 47, NL-6700 AA, Wageningen, Netherlands.

*To whom correspondence should be addressed. E-mail: milena.holmgren@wur.nl

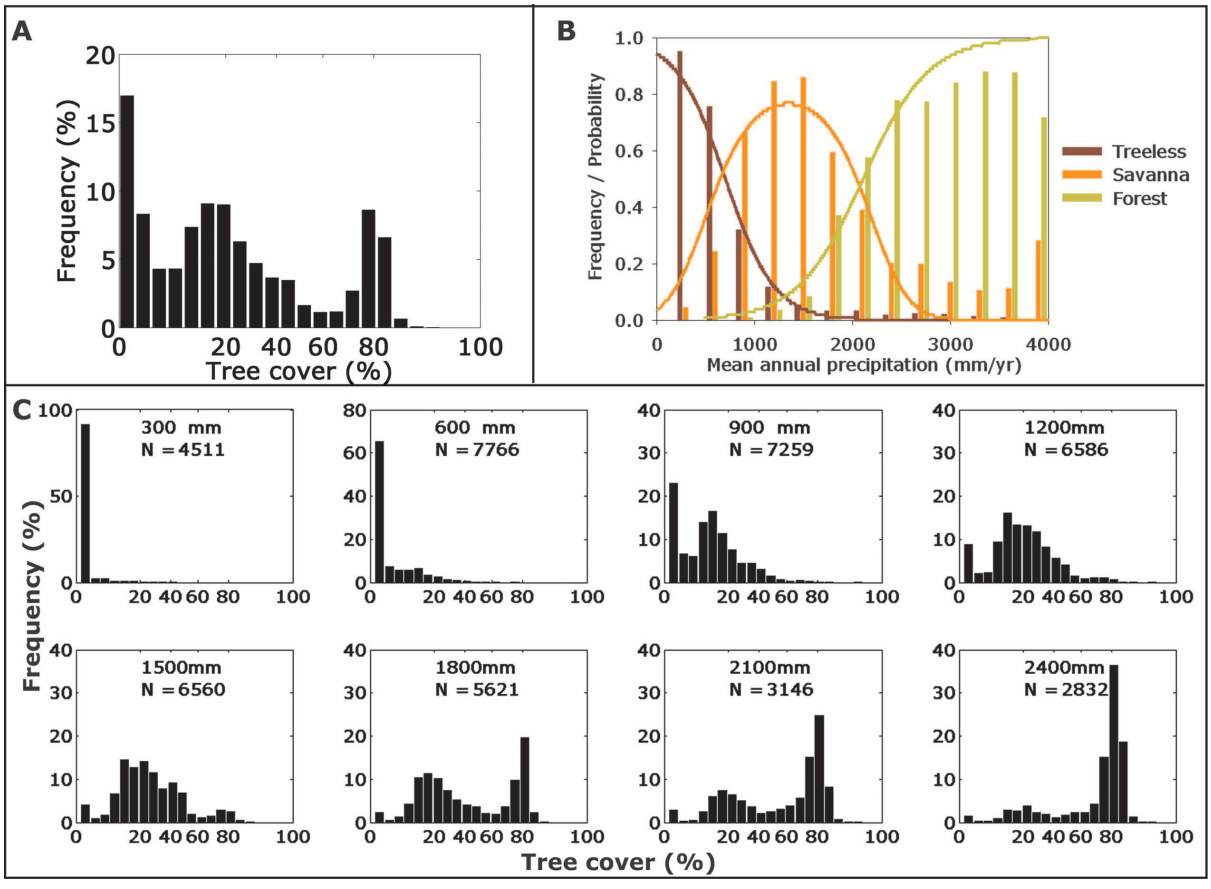

Fig. 1. Tree cover distribution in tropical and subtropical regions of Africa, Australia, and South America. (**A**) Tri-modal relative frequency distribution of tree cover (*T*) indicating three distinct underlying states: forest, savanna, and treeless, defined for further analyses as $T \geq 60\%$, $5\% \leq T < 60\%$, and $T < 5\%$, respectively (*12*). (**B**) The probability of being in each of the states as a function of the mean annual precipitation. Bars represent the relative frequency of the three vegetation types in rainfall classes. Curves represent logistic regression models (table S3). (**C**) Frequency distributions of tree cover at different precipitation levels, illustrating the fact that distinct vegetation types persist despite the overall shift from treeless to forest with increasing precipitation. In (A) and (C), the percent of tree cover has been arcsine-transformed.

Fig. 2. Tree cover (untransformed) in 1-km^2 grid cells as a function of the mean annual precipitation for (**A**) Africa, (**B**) Australia, (**C**) South America, and (**D**) intercontinental data sets [between 35°S and 15°N (*12*)]. Although the precipitation distribution and forest abundance vary between continents, the statistical relationships of tree cover to precipitation are quite similar (fig. S2).

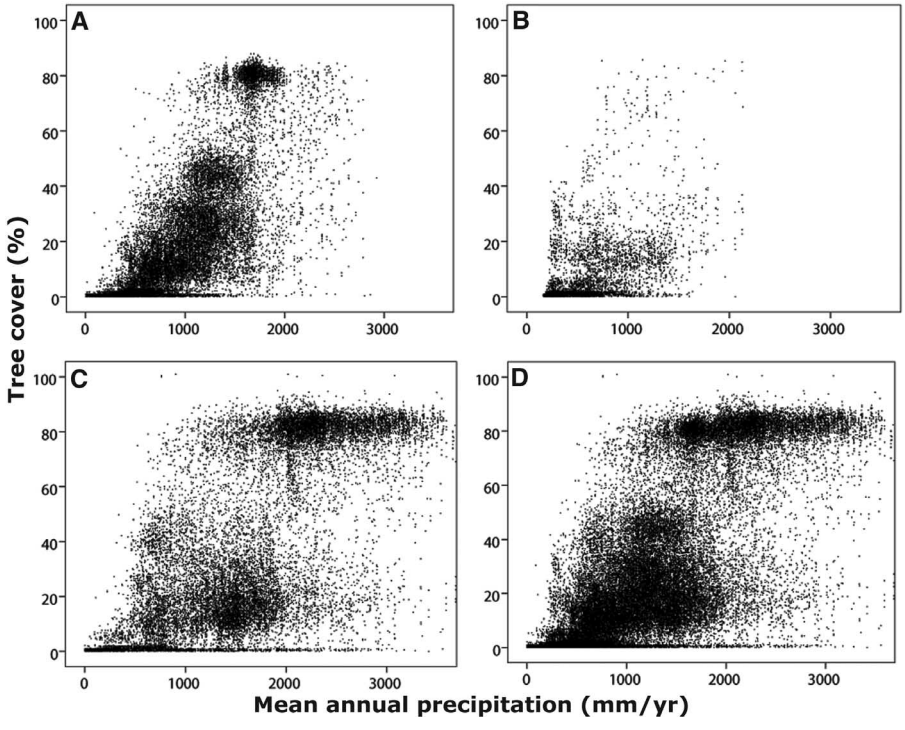

analyzed the MODIS (Moderate-Resolution Imaging Spectroradiometer) set of remotely sensed estimates of tree cover in 1-km^2 blocks in tropical and subtropical zones of Africa, Australia, and South America. We relate these patterns to precipitation (*12*), which is a major driver of past (*13*) and recent (*14*) shifts in the extension of tropical forests and savannas.

Taking the entire data set together, the frequency distribution of tree cover (Fig. 1A) is strikingly tri-modal (table S1), implying that there are three distinct underlying states: forest, savanna, and treeless. A closer look at tree distributions for different precipitation ranges (Fig. 1C) shows that although there is an overall increase of average tree cover with precipitation, the distinct character of the three states remains. Indeed, the characteristic tree cover of savanna (around 20%) and of forest (around 80%) remains remarkably constant over a wide range of rainfall levels. Thus, rather than a gradual increase in tree cover with precipitation, we see a shifting probability of being in either of the three distinct states. Defining cutoff levels of 5 and 60% tree cover for treeless and forest states, respectively (fig. S1), we can compute the probability of being in each of the states as a function of precipitation (Fig. 1B). Although continents differ widely in their rainfall range and forest abundance (Fig. 2), we find little difference between the continents in the way in which the probability of finding forest or savanna varies with precipitation (fig. S2), suggesting that the probability of finding the three alternative states varies in a fairly universal way with rainfall for tropical and subtropical regions. The most conspicuous deviation is a relative lack of forest in high-rainfall places in Australia, which is most likely explained by their relatively long dry season (*15*).

The patterns suggest a double hysteresis of tree cover in response to rainfall (Fig. 3). This can be inferred in a formal way from the data, assuming the distribution of states to result from the interplay between stochastic processes and the dynamics of an underlying deterministic system (*16*). The diminishing frequency at which the three states occur toward the end of their precipitation range corresponds to a decrease in the size of the basin of attraction of the states toward the bifurcation points (*B*), where the stability ends through a collision with the unstable (dashed) equilibria. The resilience, defined as the capacity to recover from perturbations (*17*, *18*), declines toward such tipping points. For instance, approaching the bifurcation point $B_{F,S}$ at which a forest-savanna transition is inevitable, the basin of attraction of the forest state shrinks while the attraction basin around the savanna state is growing. As a consequence, the critical loss of tree cover beyond which forest is expected to shift toward a savanna state becomes smaller in the vicinity of this bifurcation point.

The inferred shapes of the basins of attraction show how the resilience of the different states changes with precipitation. Another obvious indicator of resilience of a state for a given annual precipitation level is simply the fraction of sites that are in that state. Our logistic regression models predict that fraction as a function of rainfall (Fig. 1B). One straightforward application is the mapping of estimated resilience for current biomes. In this interpretation, a currently forested site, for instance, has a low resilience if, given its rainfall, the site would be much more likely to be in a savanna or treeless state. One can imagine that such forests most easily shift to a contrasting state with fewer trees in response to perturbations such as drought or logging. As an example of such a resilience map, consider the estimated forest resilience for the South American continent (Fig. 4). The low predicted resilience of forest in the central-eastern and southeastern Amazon basin coincides with human pressures in the arc of deforestation. These areas are precisely the regions with the highest risk of enhanced drought in future climate scenarios (*19*). For savanna, resilience decreases toward the drier end, where the chances of turning into a treeless state are larger, but also toward the wetter end, where a forested state seems a more likely alternative. At the latter sites it seems reasonable to assume that forests could be restored relatively easily. A full set of resilience maps for the three continents can be found in (*12*).

To interpret these results in terms of vulnerability and management options it is important to understand the causes of patterns. Many studies have related tree cover to abiotic and biotic drivers (*1*–*11*) as well as social drivers (*19*–*22*), all of which will probably affect the resilience of the

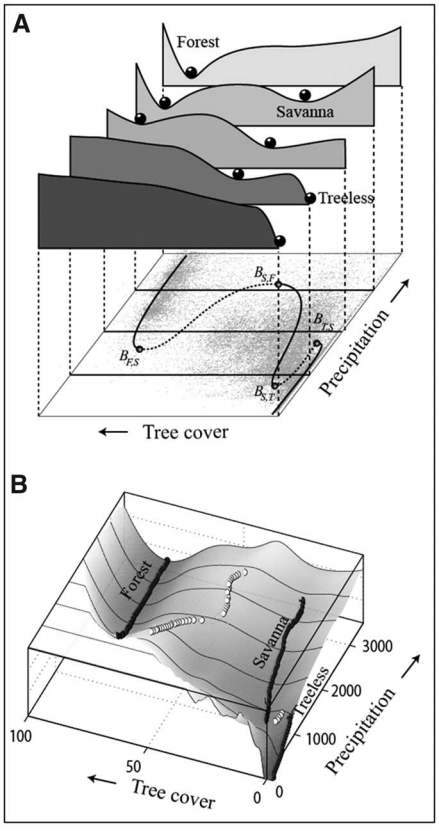

Fig. 3. Relationship between the resilience of tropical forest, savanna, and treeless states and mean annual precipitation (in millimeters per year). (**A**) The tree cover data (percent, bottom plane) suggest a double catastrophe-fold. Stable states correspond to solid parts of the curve on the bottom plane and to minima in the stability landscapes. Unstable equilibria correspond to the dashed parts of the curve and to hilltops in the stability landscapes. At bifurcation points (*B*), stable equilibria disappear through collision with unstable equilibria. Resilience measured as the width of the basin of attraction around a stable state diminishes toward such bifurcation points. (**B**) Potential landscapes as computed directly from the data. Stable states (solid dots) are minima and the unstable equilibria (open dots) are maxima at a given precipitation level. A three-dimensional animation is available at (*12*).

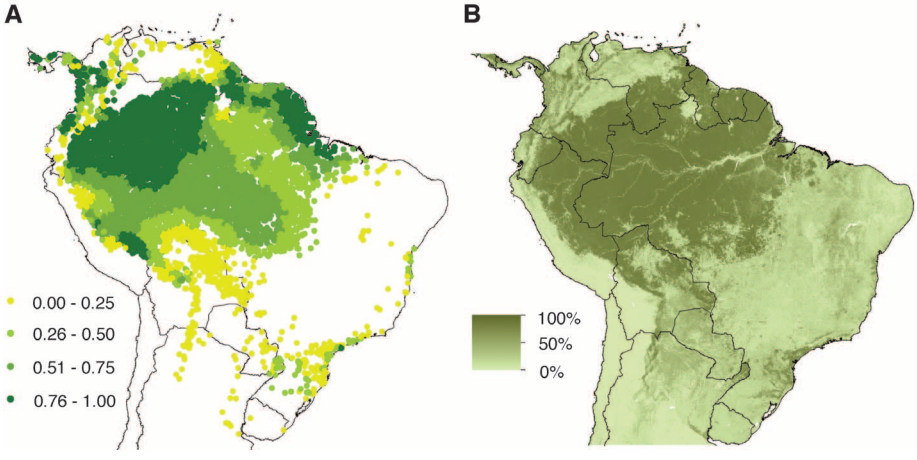

Fig. 4. Forest resilience for South America. (**A**) Resilience of remaining forest expressed as the probability of finding forest at the local mean annual precipitation level, computed with the global logistic regression model depicted in Fig. 2B. Forest with low resilience (yellow dots) is predicted to be most likely to turn into a savanna or treeless state. (**B**) Current distribution of tree density obtained from remote sensing (*12*). Resilience maps of forest, savanna, and treeless states for South America, Africa, and Australia can be found in (*12*).

different states. An important pattern is the conspicuous rarity of places with roughly 60 or 5% tree cover. Our interpretation is that these specific situations are unstable, and this can only be explained from positive feedbacks (*17*). Fire might play a role in the instability around 60% tree cover. It can promote the openness of savanna when grasses produce sufficient flammable fuel (*3*, *21*, *23*), but once tree cover becomes sufficiently dense, inhibition of grass growth and the resulting fires could lead to a self-propagating shift to a closed forest (*3*, *4*, *9*, *15*). The instability at very low tree cover might be related to a positive feedback, promoting further tree colonization due to facilitative amelioration of the stressors that would prevent tree seedling establishment in an entirely grassy or barren state (*1*, *24*).

The multistability suggested by our results has practical implications. For instance, deforestation to the unstable threshold of 60% tree cover might induce a self-propagating shift to an open savanna over a range of rainfall levels. On the other hand, exceptionally wet years related, for example, to strong El Niño–Southern Oscillation events could enhance the probability of a shift to higher tree cover (*25*), implying a potential window of opportunity for restoration efforts to help tip the balance (*26*). Insights into the particular ways in which drivers such as herbivores, fire, soil biota, and nutrients interact to affect tree dynamics (*1*–*11*, *23*, *25*, *26*) will be essential to design practical guidelines for managing these complex systems.

Because tree cover can substantially enhance rainfall in some parts of the world (*22*, *27*–*30*), an interactive vegetation-climate system may sometimes have alternative stable states even if vegetation by itself does not (*8*, *22*, *29*, *30*). Because our analysis refers to current rainfall distributions, it will not reveal such hysteresis resulting from vegetation-climate coupling. A corollary is that our analysis does not detect situations of low resilience related to a possible collapse of a rainfall pattern that depends on tree cover. However, coupled vegetation-climate models focusing on this issue have so far neglected the possibility of intrinsic vegetation hysteresis. Our results pave the way for a new generation of such models, combining local and regional nonlinearities. Constraining the character of the local hysteresis requires further work, because our current data combine sites that differ in aspects such as topography, rainfall variability, soil characteristics, and human pressures, thus enlarging the range of rainfall levels over which states are found.

Although more-detailed studies are essential to understand dynamics in different regions, our analysis shows that global patterns may be used to infer resilience. Such empirical approaches are essential because it is becoming clear that accurate mechanistic models to predict tipping points are currently beyond our reach (*18*), and determining the resilience of complex systems to critical transitions remains one of the most challenging problems in environmental science today (*17*, *18*).

References and Notes

1. J. I. House, S. Archer, D. D. Breshears, R. J. Scholes, *J. Biogeogr.* **30**, 1763 (2003).
2. F. I. Woodward, M. R. Lomas, C. K. Kelly, *Philos. Trans. R. Soc. London Ser. B* **359**, 1465 (2004).
3. W. J. Bond, *Annu. Rev. Ecol. Evol. Syst.* **39**, 641 (2008).
4. M. J. Hill, N. P. Hanan, Eds., *Ecosystem Function in Savannas: Measurements and Modeling at Landscape to Global Scales* (CRC Press, Boca Raton, FL, 2011).
5. M. Sankaran *et al.*, *Nature* **438**, 846 (2005).
6. A. C. Staver, S. Archibald, S. Levin, *Ecology* **92**, 1063 (2011).
7. H. T. Dublin, A. R. E. Sinclair, J. Mcglade, *J. Anim. Ecol.* **59**, 1147 (1990).
8. L. D. L. Sternberg, *Glob. Ecol. Biogeogr.* **10**, 369 (2001).
9. L. Warman, A. T. Moles, *Landscape Ecol.* **24**, 1 (2009).
10. G. Bucini, N. P. Hanan, *Glob. Ecol. Biogeogr.* **16**, 593 (2007).
11. R. J. Williams, G. A. Duff, D. M. J. S. Bowman, G. D. Cook, *J. Biogeogr.* **23**, 747 (1996).
12. See supporting material on *Science* Online.
13. F. E. Mayle, R. P. Langstroth, R. A. Fisher, P. Meir, *Philos. Trans. R. Soc. London Ser. B* **362**, 291 (2007).
14. D. M. J. S. Bowman, B. P. Murphy, D. S. Banfai, *Landscape Ecol.* **25**, 1247 (2010).
15. A. C. Liedloff, G. D. Cook, *Ecol. Modell.* **201**, 269 (2007).
16. V. N. Livina, T. M. Lenton, *Geophys. Res. Lett.* **34**, L03712 (2007).
17. M. Scheffer, *Critical Transitions in Nature and Society* (Princeton Univ. Press, Princeton, NJ, 2009).
18. M. Scheffer *et al.*, *Nature* **461**, 53 (2009).
19. Y. Malhi *et al.*, *Science* **319**, 169 (2008).
20. W. F. Laurance *et al.*, *J. Biogeogr.* **29**, 737 (2002).
21. D. C. Nepstad, C. M. Stickler, B. Soares-Filho, F. Merry, *Philos. Trans. R. Soc. London Ser. B* **363**, 1737 (2008).
22. C. A. Nobre, L. D. Borma, *Curr. Opin. Sust.* **1**, 28 (2009).
23. S. I. Higgins *et al.*, *Ecology* **88**, 1119 (2007).
24. M. Holmgren, M. Scheffer, M. A. Huston, *Ecology* **78**, 1966 (1997).
25. M. Scheffer, E. H. van Nes, M. Holmgren, T. Hughes, *Ecosystems (N. Y.)* **11**, 226 (2008).
26. M. Holmgren, M. Scheffer, *Ecosystems (N. Y.)* **4**, 151 (2001).
27. E. A. B. Eltahir, R. L. Bras, *Adv. Water Resour.* **17**, 101 (1994).
28. R. Avissar, D. Werth, *J. Hydrometeorol.* **6**, 134 (2005).
29. M. D. Oyama, C. A. Nobre, *J. Clim.* **17**, 3203 (2004).
30. V. Brovkin, M. Claussen, V. Petoukhov, A. Ganopolski, *J. Geophys. Res. Atmos.* **103**, 31613 (1998).

Acknowledgments: This research was partly funded by the European Research Council–Early Warning grant and Spinoza award received by M.S. The data reported in this paper are extracted as described in the supporting online material from the publicly available sites of MODIS (www.glcf.umd.edu/data/vcf/) and the Climatic Research Unit (www.cru.uea.ac.uk/cru/data/hrg/).

Supporting Online Material

www.sciencemag.org/cgi/content/full/334/6053/232/DC1
SOM Text
Figs. S1 to S3
Tables S1 to S3
References (*31*–*33*)
Movie S1

4 July 2011; accepted 6 September 2011
10.1126/science.1210657

The *Escherichia coli* Replisome Is Inherently DNA Damage Tolerant

Joseph T. P. Yeeles and Kenneth J. Marians*

The *Escherichia coli* DNA replication machinery must frequently overcome template lesions under normal growth conditions. Yet, the outcome of a collision between the replisome and a leading-strand template lesion remains poorly understood. Here, we demonstrate that a single, site-specific, cyclobutane pyrimidine dimer leading-strand template lesion provides only a transient block to fork progression in vitro. The replisome remains stably associated with the fork after collision with the lesion. Leading-strand synthesis is then reinitiated downstream of the damage in a reaction that is dependent on the primase, DnaG, but independent of any of the known replication-restart proteins. These observations reveal that the replisome can tolerate leading-strand template lesions without dissociating by synthesizing the leading strand discontinuously.

Encounters between the DNA replication machinery and obstacles such as DNA damage and RNA polymerase transcription complexes are thought to occur frequently under normal growth conditions (*1*–*4*). After ultraviolet irradiation of *Escherichia coli* cells, DNA replication continues past multiple lesions, generating single-stranded DNA (ssDNA) gaps in the newly synthesized DNA (*5*, *6*), implying that replication is reinitiated downstream of lesions in both the leading- and lagging-strand templates. Indeed, the replisome bypasses lagging-strand template damage with little impediment because of the discontinuous nature of lagging-strand synthesis (*7*–*9*). Leading-strand lesions may be overcome by reinitiating leading-strand synthesis downstream of damage, as the primase, DnaG, can prime the leading-strand template on a model fork structure after origin-independent replisome assembly (*10*). This model assumes that the replisome dissociates from the template after collision with the lesion and therefore requires the replication restart proteins to reload the replisome (*11*). However, the fate of the replisome after a collision with leading-strand template damage has not yet been determined.

To investigate how the replisome may overcome leading-strand template damage, we constructed a 10.4-kbp plasmid containing the *E. coli*

Molecular Biology Program, Memorial Sloan-Kettering Cancer Center, New York, NY 10065, USA.

*To whom correspondence should be addressed. E-mail: kmarians@sloankettering.edu